

EFFECTS OF IRRADIATION ON THE FRACTURE PROPERTIES
OF STAINLESS STEEL WELD OVERLAY CLADDING*

CONF-8908125--3

F. M. Haggag, W. R. Corwin,[†] and R. K. Nanstad

DE89 016265

Metals and Ceramics Division
 Oak Ridge National Laboratory
 Oak Ridge, Tennessee 37831-6151

Recd

Aug 2 1989

ABSTRACT

Stainless steel weld overlay cladding was fabricated using the submerged arc, single-wire, oscillating-electrode, and the three-wire, series-arc methods. Three layers of cladding were applied to a pressure vessel plate to provide adequate thickness for fabrication of test specimens, and irradiations were conducted at temperatures and to fluences relevant to power reactor operation. For the single-wire method, the first layer was type 309, and the upper two layers were type 308 stainless steel. The type 309 was diluted considerably by excessive melting of the base plate. The three-wire method used various combinations of types 308, 309, and 304 stainless steel weld wires, and produced a highly controlled weld chemistry, microstructure, and fracture properties in all three layers of the weld.

Postirradiation test results of all cladding specimens show that, in the test temperature range from -125 to 288°C, the yield strength increased by 40 to 5%, ductility insignificantly increased, while there was almost no change in ultimate tensile strength. All cladding exhibited ductile-to-brittle transition behavior during Charpy impact testing due to the dominance of delta-ferrite failures at low temperatures. On the upper shelf, energy was reduced up to 50% due to irradiation exposure. In addition, radiation damage resulted in 13 to 100°C shifts of the Charpy impact transition temperature at the 41-J level. Furthermore, irradiation exposure of 12.5-mm-thick compact specimens (0.5TCS), from the three-wire cladding to an average fluence of 2.41×10^{19} neutrons/cm² (>1 MeV), resulted in decreases in the initiation ductile fracture toughness,

*Research sponsored by the Office of Nuclear Regulatory Research, U.S. Nuclear Regulatory Commission, under Interagency Agreement DOE 1886-8011-9B with the U.S. Department of Energy under contract DE-AC05-84OR21400 with Martin Marietta Energy Systems, Inc.

[†]Engineering Technology Division.

The submitted manuscript has been authored by a contractor of the U.S. Government under contract No. DE-AC05-84OR21400. Accordingly, the U.S. Government retains a nonexclusive, royalty-free license to publish or reproduce the published form of this contribution, or allow others to do so, for U.S. Government

DISTRIBUTION OF THIS DOCUMENT IS UNLIMITED

DISCLAIMER

This report was prepared as an account of work sponsored by an agency of the United States Government. Neither the United States Government nor any agency thereof, nor any of their employees, makes any warranty, express or implied, or assumes any legal liability or responsibility for the accuracy, completeness, or usefulness of any information, apparatus, product, or process disclosed, or represents that its use would not infringe privately owned rights. Reference herein to any specific commercial product, process, or service by trade name, trademark, manufacturer, or otherwise does not necessarily constitute or imply its endorsement, recommendation, or favoring by the United States Government or any agency thereof. The views and opinions of authors expressed herein do not necessarily state or reflect those of the United States Government or any agency thereof.

J_{IC} , and the tearing modulus in the test temperature range from -125 to 288°C.

This is in agreement with the reduction in both the CVN upper-shelf energy and the lateral expansion.

INTRODUCTION

The ability of stainless steel cladding to improve the fracture behavior of an operating nuclear reactor pressure vessel, particularly during certain overcooling transients, may depend greatly on the properties of the irradiated cladding.¹ Therefore, weld overlay cladding irradiated at temperatures and to fluences relevant to power reactor operation was examined. Two weld cladding procedures were chosen for the two phases of this study, namely, the single-wire oscillating submerged-arc and the three-wire series-arc. The primary differences between these procedures are in the heat input and the resulting amounts of base metal dilution of the stainless steel cladding. In the first phase, previously reported in detail,²⁻⁵ Charpy V-notch (CVN) impact and tensile specimens from a three-layer stainless steel weld overlay fabricated using the single-wire procedure were irradiated to 2×10^{19} neutrons/cm² (>1 MeV) at 288°C. Cladding from the upper weldment layers, typical of good quality pressure vessel cladding, exhibited very little irradiation-induced degradation. However, ductile-to-brittle transition behavior, caused by temperature dependent failure of the residual delta-ferrite, was observed during impact testing. In contrast, specimens from the first weldment layer, which also exhibited transition type behavior, were markedly embrittled. The cause of the embrittlement was determined to be high radiation sensitivity of the atypical microstructure resulting from excessive (≈50%) base metal dilution of the first weldment layer. (Good commercial single-wire cladding normally contains 15-25% dilution of base metal.)

In the second phase,⁶⁻⁸ a commercially produced three-wire series-arc stainless steel cladding was evaluated under similar irradiation (except for the high-fluence specimens) and testing conditions as in the first phase. The results of tensile, CVN impact, and fracture toughness tests are reported here and compared with the properties of the unirradiated material.

MATERIALS

PHASE 1: SINGLE-WIRE CLADDING

The specimens were all taken from a single laboratory weldment fabricated by the automated single-wire oscillating submerged arc procedure. The welding wires for both types of 308 and 309 stainless steel were 4 mm in diameter and were chosen to be representative of cladding formerly applied in industry. The cladding was deposited on plates that were 114 mm thick by 406 mm wide by 914 mm long to minimize distortion and to provide adequate heat sink. The clad plates were then postweld heat treated (PWHT) at 621°C for 40 h to represent commercial practice. More details of welding procedure and parameters and cladding microstructure are given in ref. 5. The three layers of cladding were applied to provide adequate cladding thickness (≈ 20 mm) to obtain test specimens. This contrasts with typical commercial practice, in which a single layer of overlay approximately 5 mm thick is applied by either multiple wire or strip-cladding submerged arc procedures. The material compositions of each layer of weld metal are given in Table 1. Subsequent metallographic examination showed that the upper layer appeared typical of good quality light water reactor (LWR) stainless steel weld overlay, whereas the lower layer had incurred excessive ($\approx 50\%$) dilution as a result of base metal melting during welding.

To examine the effect of the varying microstructures, two sets of tensile and Charpy V-notch specimens were carefully fabricated to be contained as fully as possible within either the upper two layers (nominally type 308 specimens) or the lower layer (nominally type 309 specimens) (Fig. 1). All specimens were fabricated with the specimen axis parallel to the welding direction. The Charpy specimens were notched on the surface parallel to and nearer the base metal in all cases. Ferrite numbers were measured on the finished Charpy specimens with a Ferrite Scope, which locally measures the percentage of ferromagnetic material in the sample. The nominally type 308 specimens consistently had ferrite numbers of 2 to 6 (corresponding roughly to percentages of ferrite), as did the portion of nominally type 309 specimens composed of upper weld pass layers. The notched side of the nominally type 309 specimens closest to the base metal interface

exhibited a wide range of ferrite numbers from 2 to greater than 30 (off scale), reflecting the large amounts of the ferritic base metal melted by the first weld pass.

PHASE 2: THREE-WIRE CLADDING

The specimens were taken from commercially produced stainless steel cladding overlaid on a pressure vessel steel plate. The base material, HSST Plate 012B, was a 178-mm-thick (7-in.) plate of A533 grade B class 1 steel. Three layers of cladding were applied to provide adequate thickness (≈ 20 mm) for fabrication of the test specimens. The three-wire series-arc procedure, developed by Combustion Engineering, Inc. (CE), Chattanooga, Tennessee, produced a highly controlled weld chemistry, microstructure, and fracture properties in all three layers of the weld.

The three-wire series-arc weld overlay cladding procedure of this work was representative of that used in older nuclear pressure vessels. This method has generally been replaced by strip cladding processes. Various combinations of type 308, 309, and 304 stainless steel wires were used in the three layers of cladding. Table 2 provides the chemical compositions for each layer of the weld overlay. The cladding was given an initial postweld heat treatment (PWHT) by CE of 593°C for 10 h, notably less than the PWHT of 621°C for 40 h typically given to the cladding of a pressurized water reactor (PWR) during fabrication. The cladding received this milder PWHT at CE due to requirements of the clad-beam program with which this irradiation program material was concurrently fabricated. To bring the heat treatment of the cladding into the range more typically given PWRs, additional PWHT was performed. Calculations were made using the following tempering parameter (TP) (ref. 9):

$$TP = T(20 + \log t) \times 10^{-3} ,$$

where T = temperature (K) and t = time (h). According to this method, the PWHT given the cladding at CE was calculated to be equivalent to a time of 2.2 h at 621°C. Therefore, an additional 37.8 h of PWHT at 621°C was given the cladding at ORNL to approximate the typical 40-h period.

The delta-ferrite content was monitored for all three layers of the cladding with a Fischer Ferrite scope. The ferrite numbers varied from 7.5 to 10 throughout the three layers of the cladding. The microstructure of this cladding (Fig. 2) reveals a distribution of delta-ferrite in an austenitic matrix, quite typical of microstructures seen in good practice commercial weld overlay cladding in reactor pressure vessels.²⁻⁵

IRRADIATION HISTORY

PHASE 1: SINGLE-WIRE CLADDING

The specimens were irradiated by Materials Engineering Associates in the core of the 2-MW pool reactor (UBR) at the Nuclear Science and Technology Facility, Buffalo, New York. Two separate capsules were used, one each for the type 308 and 309 stainless steel specimens. The capsules were instrumented with thermocouples and dosimeters and were rotated 180° once during the irradiation for fluence balancing. The capsule containing the type 308 specimens reached an average fluence ± 1 standard deviation of 2.09×10^{19} neutrons/cm² (>1 MeV) $\pm 10\%$ during 679 h of irradiation. The capsule containing the type 309 specimens reached an average fluence of 2.02×10^{19} neutrons/cm² (>1 MeV) $\pm 5\%$ in 508 h. The fluences are for a calculated spectrum based on Fe, Ni, and Co dosimetry wires. Temperatures were maintained at $288 \pm 14^\circ\text{C}$ except for the initial week of irradiation. During that time, temperatures as low as 263°C were recorded for the type 308 specimens.

PHASE 2: THREE-WIRE CLADDING

The CVN and tensile specimens were irradiated in two capsules [with target fluences of 2 and 5×10^{19} neutrons/cm² (>1 MeV)] by Materials Engineering Associates (MEA) in the core of the 2-MW pool reactor (UBR) at the Nuclear Science and Technology Facility, Buffalo, New York. Each capsule contained 20 CVN and 6 miniature tensile (MT) specimens and was instrumented with thermocouples and dosimeters. Each capsule was rotated 180° at least once during its irradiation exposure for side-to-side fluence balancing. Irradiation

temperatures were maintained at $288 \pm 11^\circ\text{C}$. The average fluence for the first capsule was 2.14×10^{19} neutrons/cm² (>1 MeV) $\pm 8\%$ following 631 h of irradiation. The second capsule reached an average fluence of 5.56×10^{19} neutrons/cm² (>1 MeV) $\pm 5\%$ in 1605 h. These fluences are for a calculated spectrum based on Fe, Ni, and Co dosimetry wires. Eight 12.7-mm-thick compact specimens (0.5TCS) were irradiated in a third capsule to an average fluence of 2.41×10^{19} neutrons/cm² (>1 MeV) $\pm 3\%$ following 637 h of irradiation.

RESULTS AND DISCUSSION

PHASE 1: SINGLE-WIRE CLADDING

Tensile testing was conducted at room temperature, 149°C , and 288°C . Irradiation increased the yield strength of the type 309 specimens by 30 to 40%, whereas the increase of the type 308 specimens was only 5 to 25%. Surprisingly, the total elongation and reduction in area of both materials increased during irradiation. The effect of irradiation on the Charpy impact properties of the type 308 weld metal representative of typical weld overlay cladding was relatively small (Fig. 3). Only a very slight upward shift in transition temperature (15°C) and drop in upper-shelf (<10%) were observed.

The interpretation of the impact results of the nominally type 309 specimens is more complicated. Since the type 309 weld pass was not thick enough to obtain specimens composed entirely of type 309 weld metal, a portion of all specimens nominally called type 309 is indeed type 308. Macrographs of the irradiated specimens fracture surfaces show that over the range of the full Charpy curve, the portion composed of type 309 weldment remains bright and faceted. The remainder of the fracture surface, composed of upper cladding layers of type 308 weld metal, exhibits the same behavior seen in fully type 308 specimens. In the nominally type 309 specimens, interpreting the Charpy impact curves demands that the dual fracture properties of the type 308 and 309 portions of the material be taken into consideration. Examination of the fracture surfaces showed clearly that the type 308 weld metal has a lower transition temperature than does the type 309. Examining the impact data reveals a bimodal population related to the amount of the tougher type 308 weld metal present in the sample. The more

type 308 in the specimen, the lower the apparent transition temperature of the specimen. Hence, the unirradiated and irradiated specimens were categorized into low- and high-energy populations based on the percentage of type 308 weld metal measured visually on the fracture surface of each specimen. The most appropriate criteria for separating the low-energy populations were arbitrarily chosen to be less than 70 and 80% type 308 weld metal for the unirradiated and irradiated data sets, respectively, because these produced the most distinct difference between the data sets.

The effect of irradiation on type 309 cladding was appreciable (Fig. 4). Both energy populations experienced large drops in upper-shelf energy of up to 50% and shifts in transition temperature of up to 100°C. The extensive toughness degradation seen in the type 309 material as compared with little in the type 308 is probably due to the higher fraction of ferritic phases in the type 309 resulting from the excessive base metal dilution and their intrinsically higher radiation sensitivity.

PHASE 2: THREE-WIRE CLADDING

Unirradiated Results

Tensile tests were conducted in the temperature range of -125 to 288°C. The effect of specimen orientation on tensile properties was insignificant (Fig. 5). Hence, only MT specimens with their axes oriented in the longitudinal (rolling and welding) direction were irradiated at 288°C to the two fluence levels mentioned earlier. The cladding exhibits an extremely rapid rise in tensile strength below about 0°C as shown in Fig. 5. This figure also shows that the ductility increases from high temperatures to a peak near 0°C, then decreases at lower temperatures. At 0°C and above, the fracture mode of the tensile specimens is strain controlled and matrix dominated. As the strength increases with decreasing temperature, void coalescence requires greater strain resulting in higher measured elongation. At temperatures below 0°C, however, the ferrite phase begins to dominate in a stress-controlled manner and its propensity for cleavage failure leads to lower specimen total strain to failure and, thus, reduced total elongation.

Charpy impact specimens were machined in the L-T, L-S, T-L, and T-S orientations. The L-orientation in all the cladding work here represents the welding direction as well as the rolling direction of the base plate. The four specimen orientations were chosen to simulate the possibilities of crack extension in the axial and circumferential orientations, both across (T-orientation) and through (S-orientation) the cladding of a pressure vessel. All three-wire cladding specimens exhibited ductile-to-brittle transition behavior (similar to that of single-wire cladding in Fig. 4 and refs. 2-5) during impact testing, due to the dominance of delta-ferrite failures at low temperatures. The test results also show relatively small variations of Charpy impact toughness in four orientations [Fig. 6(b)]. Hence, CVN irradiated specimens were machined only from the cladding with their notches in the L-S orientation since this orientation exhibited a typical transition temperature as well as a slightly lower upper-shelf energy. The CVN data scatter in the four orientations was typical to that shown in Fig. 6(a).

The fracture appearance macroscopically did not change substantially from the upper to lower shelf as shown in Fig. 7. These CVN specimens (unirradiated, L-S orientation), whose test results are shown in Fig. 6(a), were further examined in the scanning electron microscope. The specimen tested at 100°C absorbed 80 J and fractured in a fully ductile manner by microvoid coalescence. The spherical particles that initiated the dimples were readily visible on the fracture surface. In contrast, the specimen tested at -100°C absorbed only 20 J and fractured in a much more brittle mode. The fracture surface of this specimen contained areas of cleavage associated with the ferrite phase (Fig. 8). Also present were smooth regions believed to be associated with the ferrite-austenite interfaces, indicating that fracture occurred by interphase separation. Some isolated patches of dimples and their initiating particles were also present. Metallographic studies and scanning electron microscopic examination demonstrated that the fracture of stainless steel cladding is matrix controlled on the upper shelf and ferrite controlled at lower temperatures.⁵

The unirradiated and irradiated 12.7-mm-thick compact specimens (0.5TCS) were machined in the L-S orientation; the L-orientation here represents the rolling direction for the base metal (A533 grade B class 1 steel) as well as the welding direction for the three-wire stainless steel weld overlay cladding.

Since the cladding thickness was approximately 20 mm, the specimens were machined carefully such that their back surfaces, perpendicular to the crack plane, were parallel and close to the top surface of the cladding. This approach was necessary since the nominal total width of each specimen (1.25W) of 31.75 mm was greater than the full thickness of the cladding (20 mm), thereby assuring that the fatigue precrack and its subsequent test extension resided fully in the cladding and that only a portion of the specimen, containing the loading holes, was machined from the pressure vessel steel base metal. The specimens were tested according to ASTM Standard E 813-87 (ref. 10) using a computer-controlled unloading-compliance technique in the test temperature range of -75 to 288°C. The J-integral calculations for deformation J-integral (as recommended in ASTM Standard E 813-87) and for the modified J-integral were performed using equations similar to those given in refs. 11 and 12, respectively. The fracture toughness test results of both unirradiated and irradiated specimens are presented and discussed below.

Effect of Irradiation on Tensile Properties

The yield strength of three-wire stainless steel cladding increased due to radiation exposure. The effects were greater at room temperature and below (Fig. 9); for example, at the fluence of 2×10^{19} neutrons/cm² (>1 MeV) the yield strength increased by 9, 20, and 28% at test temperatures of 288°C, room temperature, and -125°C, respectively. At the higher fluence level of 5×10^{19} neutrons/cm² (>1 MeV), the yield strength increased by 6, 16, and 34% at the test temperatures of 288°C, room temperature, and -125°C, respectively. Hence, it can be seen that virtually all the radiation hardening occurred at the lower fluence; increasing the fluence by a factor of 2.5 did not result in further radiation hardening. The effects of irradiation on the ultimate strength were insignificant [Fig. 10(a)]. The small increase in ductility [see Fig. 10(b)] due to irradiation at 288°C could be due to thermal aging and/or radiation exposure. To separate these effects, a few tensile specimens will be aged at 288°C for 631 and 1605 h and their test results will be compared to those of irradiated specimens. It is believed that the effect of irradiation on ductility as measured by total elongation is similar to the effect of temperature as

explained earlier in the discussion of Fig. 5, i.e., irradiation hardening increases the flow stress by strengthening the austenite and ferrite phases in the stainless steel weld cladding. The ferrite phase is much more sensitive than the austenite phase to both irradiation hardening and low test temperatures. Again, at ambient temperature and above, the increased flow stress results in higher strains associated with void coalescence and leads to higher total strain to failure and thus higher total elongation. Furthermore, at temperatures below ambient, the ferrite phase, which is hardened by both irradiation and temperature, experiences localized cleavage failures. Those cleavage events reduce the total specimen strain to failure and, thus, reduce the total elongation.

Effect of Irradiation on Charpy Impact Properties

Irradiation of the three-wire stainless steel cladding specimens at 288°C to fluence levels of 2 and 5×10^{19} neutrons/cm² (>1 MeV) resulted in decreases of the CVN upper-shelf energy by 15 and 20% and increases of the 41-J transition temperature by 13 and 28°C, respectively [Fig. 11(a)]. Figure 11(b) shows that increasing irradiation from 2 to 5×10^{19} neutrons/cm² further degraded the three-wire stainless steel cladding. Irradiation also degraded the CVN lateral expansion significantly (Fig. 12). The upper-shelf lateral expansion was reduced by 43 and 41% at the low and high fluences, respectively. Furthermore, the 0.38-mm (0.015-in.) transition temperature shifts were 41 and 46°C for the low and high fluences, respectively. Lateral expansion values in the lower-shelf region were also substantially degraded by irradiation. Table 3 also provides the hyperbolic tangent curve fit results for the unirradiated and irradiated CVN test results. These results are in general agreement with those for the single-wire cladding produced with good welding practice.²⁻⁵

Effect of Irradiation on Ductile Fracture Toughness and Tearing Modulus

Results of the unirradiated and irradiated 0.5TGS fracture toughness specimens fabricated from three-wire series-arc stainless steel cladding are summarized in Table 4. Table 4 and Figs. 13 and 14 also show that irradiation

exposure to an average fluence of 2.41×10^{19} neutrons/cm² (>1 MeV) resulted in decreases in both the initiation ductile fracture toughness, J_{Ic} , and the tearing modulus at test temperatures of -75°C, room temperature, 120°C, and 288°C. This is consistent with the reductions in both the CVN upper-shelf energy and lateral expansion discussed above. However, the percent reduction in initiation toughness of the 0.5TCS specimens at high temperatures (e.g., at 288°C) is greater than that of the CVN impact energy but closer to the percent reduction of the CVN lateral expansion. Table 4 and Fig. 13 show that the initiation toughness, J_{Ic} , increased from high temperature to a peak (at about ambient temperature for unirradiated specimens and about 50°C for irradiated specimens) and then decreased at low temperatures similar to the ductile behavior shown earlier in Fig. 5. Table 4 also shows, as expected, that the tearing modulus calculated according to ref. 12 (modified J-integral calculation) was always higher than that calculated according to ref. 11 (deformation J-integral approach) for both unirradiated and irradiated materials. Unirradiated specimen A13F was not included in Figs. 14 and 15 since it was not side grooved; its results of higher (as compared to the 20% side-grooved specimens) J_{Ic} and tearing modulus were also expected. An example of the unirradiated and irradiated J-integral vs crack extension (J-R) curves for specimens tested at 120°C is shown in Fig. 15. The J_{Ic} values for the two irradiated specimens tested at -75°C were significantly lower than those for unirradiated specimens (see Table 4).

The low value of J_{Ic} (23 kJ/m²) for the irradiated specimen tested at 288°C (see Table 4 and Fig. 13) is considerably less than the lowest J_{Ic} value, 43.1 kJ/m², observed for the low upper-shelf welds tested in the HSST Second and Third Irradiation Series.¹³ It is also substantially lower than the lowest J_{Ic} value, 83.3 kJ/m², obtained for the A533 grade B class 1 plate (HSST 02) in the HSST Fourth Irradiation Series.¹⁴

CONCLUSIONS AND DESCRIPTION OF FUTURE WORK

The irradiation effects on the Charpy upper-shelf impact and transition temperature of good quality single-wire stainless steel cladding were very small. The tensile strength and ductility were improved slightly by irradiation.

Results from the highly diluted type 309 weld metal showed appreciable radiation-induced degradation of notch-impact toughness, even though both the tensile strength and ductility were improved slightly by irradiation. Although this is a single case of single-wire cladding; for known cases where welding has produced abnormal cladding with excessive dilution in operating reactors, the radiation effects on notch impact toughness may be cause for concern.

The effects of neutron irradiation on three-wire stainless steel weld cladding, prototypical of commercial light-water reactor materials, were evaluated at a wide range of test temperatures for conditions similar to those at the end of life of a pressurized water reactor. The yield strength of this cladding increased with irradiation exposure; the increase rate was appreciably higher at low temperatures (room temperature and below). However, the effects of irradiation on the ultimate tensile strength and ductility (uniform and total elongation) were insignificant.

All the unirradiated and irradiated three-wire cladding specimens exhibited ductile-to-brittle transition behavior similar to that seen previously for the single-wire cladding. Again, this was also attributed to the dominance of failure of delta-ferrite at lower temperatures. The upper-shelf energy was reduced by 15 and 20%, while the upper-shelf lateral expansion was reduced 43 and 41%, at 2.14 and 5.56×10^{19} neutrons/cm² (>1 MeV), respectively. The 41-J transition temperature shifts were 13 and 28°C for the low and high levels of fluence, respectively.

Irradiated 0.5TCS specimens tested from -75 to 288°C showed consistent decreases in both ductile initiation fracture toughness and tearing modulus in qualitative agreement with observed decreases in Charpy impact energy and lateral expansion. Extremely low resistance to ductile crack initiation was observed at the test temperature of 288°C for the irradiated cladding. Considering those results, the ability of the stainless steel cladding to enhance the structural integrity of irradiated pressure vessels clad with similar material should be investigated further.

It must be stressed that the results presented and discussed in this paper are derived from only two stainless steel cladding materials; hence, no conclusions can be drawn for different material chemistries and/or welding procedures.

Stainless steel cladding from the decommissioned West German boiling-water reactor at Gundremmingen will be examined using subsized specimen techniques to compare to our reactor data. The subsized specimens will be machined from the recently acquired four trepan cuts from the decommissioned reactor.

ACKNOWLEDGMENTS

The authors gratefully acknowledge the personnel of Materials Engineering Associates, particularly J. R. Hawthorne, for capsule fabrication and irradiation. The fractography work of D. J. Alexander is highly appreciated. We acknowledge T. N. Jones, R. L. Swain, and E. T. Manneschildt for their experimental assistance; and J. L. Bishop for preparing the manuscript. We also acknowledge the support of our technical monitor, Michael E. Mayfield, the Materials Engineering Branch Chief, Charles Z. Serpan, Jr., and the U.S. Nuclear Regulatory Commission.

REFERENCES

1. W. R. Corwin, *Assessment of Radiation Effects Relating to Reactor Pressure Vessel Cladding*, NUREG/CR-3671 (ORNL-6047), Martin Marietta Energy Systems, Inc., Oak Ridge Natl. Lab., July 1984.
2. W. R. Corwin, R. G. Berggren, and R. K. Nanstad, *Charpy Toughness and Tensile Properties of a Neutron-Irradiated Stainless Steel Submerged Arc Weld Cladding Overlay*, NUREG/CR-3927 (ORNL/TM-9309), Martin Marietta Energy Systems, Inc., Oak Ridge Natl. Lab., September 1984.
3. W. R. Corwin, R. G. Berggren, and R. K. Nanstad, "Fracture Properties of a Neutron-Irradiated Stainless Steel Submerged Arc Weld Cladding Overlay," pp. 26-47 in *Proceedings of the U.S. Nuclear Regulatory Commission Twelfth Water Reactor Safety Research Information Meeting, held at Gaithersburg, Maryland, October 22-26, 1984*, NUREG/CP-0058, Vol. 4, January 1985.
4. W. R. Corwin, R. G. Berggren, and R. K. Nanstad, "Charpy Toughness and Tensile Properties of a Neutron-Irradiated Stainless Steel Submerged-Arc Weld Cladding Overlay," pp. 951-71 in *Effects of Radiation on Materials*, ASTM STP 870, proceedings of the Twelfth International Symposium, Williamsburg, Va., F. A. Garner and J. S. Perrin, Eds., American Society for Testing and Materials, Philadelphia, 1985.
5. W. R. Corwin, R. G. Berggren, and R. K. Nanstad, "Fracture Behavior of a Neutron-Irradiated Stainless Steel Submerged Arc Weld Cladding Overlay," *Nucl. Eng. Des.* 89, 199-221 (1985).
6. F. M. Haggag, W. R. Corwin, D. J. Alexander, and R. K. Nanstad, "Effects of Irradiation on Strength and Toughness of Commercial LWR Vessel Cladding," pp. 177-93 in *Proceedings of the U.S. Nuclear Regulatory Commission Fifteenth Water Reactor Safety Information Meeting, held at Gaithersburg, Maryland, October 26-29, 1987*, NUREG/CP-0091, Vol. 2, February 1988.

7. F. M. Haggag and S. K. Iskander, "Results of Irradiated Cladding Tests and Clad Plate Experiments," pp. 355-69 in *Proceedings of the U.S. Nuclear Regulatory Commission Sixteenth Water Reactor Safety Information Meeting, held at Gaithersburg, Maryland, October 24-27, 1988*, NUREG/CP-0097, Vol. 2, March 1989.

8. F. M. Haggag, W. R. Corwin, D. J. Alexander, and R. K. Nanstad, "Tensile and Charpy Impact Behavior of an Irradiated Three-Wire Series-Arc Stainless Steel Cladding," to be published in proceedings of ASTM 14th International Symposium on Effects of radiation on Materials, Andover, Mass., June 27-30, 1988.

9. R. W. Swindeman, R. K. Nanstad, J. F. King, and W. J. Stelzman, *Effect of Tempering on the Strength and Toughness of 2 1/4 Cr-1 Mo Steel Weldments*, ORNL/TM-9307, Martin Marietta Energy Systems, Inc., Oak Ridge Natl. Lab., October 1984.

10. ASTM E 813-87, "Standard Test Method for J_{Ic} , A Measure of Fracture Toughness," pp. 686-700 in *Annual Book of ASTM Standards*, Vol. 03.01, American Society for Testing and Materials, Philadelphia, 1988.

11. ASTM E 1152-87, "Standard Test Method for Determining J-R Curves," pp. 800-810 in *Annual Book of ASTM Standards*, Vol. 03.01, American Society for Testing and Materials, Philadelphia, 1988.

12. H. A. Ernst, "Materials Resistance and Instability Beyond J-Controlled Crack Growth," pp. 191-213 in *Elastic-Plastic Fracture*, Vol. I, STP 803, C. F. Shih and J. P. Gudas, Eds., American Society for Testing and Materials, Philadelphia, 1983.

13. A. L. Hiser, F. J. Loss, and B. H. Menke, *J-R Curve Characterization of Irradiated Low Upper Shelf Welds*, NUREG/CR-3506 (MEA-2028), Materials Engineering Associates, Inc., April 1984.

14. J. J. McGowan, R. K. Nanstad, and K. R. Thoms, *Characterization of Irradiated Current-Practice Welds and A533 Grade B Class 1 Plate for Nuclear Pressure Vessel Service*, NUREG/CR-4880, Vol. 1 (ORNL-6484/V1), Martin Marietta Energy Systems, Inc., Oak Ridge Natl. Lab., July 1988.

Table 1. Chemical composition of single-wire stainless steel weld clad overlay used in Phase 1 of the Seventh Irradiation Series

Layer	Content, ^a wt %												
	C	Cr	Ni	Mo	Mn	Si	Co	Cu	V	Al	Ti	P	S
Lower	0.145	13.46	6.90	0.47	1.47	0.56	0.066	0.14	0.02	0.014	<0.005	0.018	0.01
Middle	0.081	18.52	8.81	0.27	1.47	0.70	0.092	0.10	0.04	0.010	<0.005	0.021	0.01
Upper	0.065	20.01	9.36	0.21	1.49	0.76	0.100	0.09	0.04	0.16	0.006	0.022	0.01

^aBalance Fe, with Nb < 0.01; Ta < 0.01; As < 0.03; and B < 0.001 for all layers.

Table 2. Chemical composition of the three-wire stainless steel weld clad overlay used in Phase 2 of the Seventh Irradiation Series

Layer	Content, ^a wt %											
	C	Cr	Ni	Mo	Mn	Si	Co	Cu	V	P	S	
Lower	0.052	19.75	9.75	0.18	1.59	0.63	0.03	0.07	0.03	0.016	0.014	
Middle	0.049	19.38	9.18	0.23	1.28	0.78	0.07	0.36	0.06	0.023	0.017	
Upper	0.049	19.34	9.04	0.23	1.34	0.82	0.08	0.39	0.06	0.023	0.017	

^aBalance Fe, with Nb < 0.01; Ti < 0.01; and N < 0.057 for all layers.

Table 3. Charpy impact test results for stainless steel three-wire series-arc cladding

Orientation ^a	Fluence, n/cm ² (>1 MeV)	Transition temperature criterion (°C)			Energy (J)		Lateral expansion (mm)	
		41 J	68 J	0.38 mm	Upper shelf	Lower shelf	Upper	Lower
L-S	0	-41	6	-57	82	13	1.15	0.25
L-S	2 × 10 ¹⁹	-28	56	-16	70	9	0.65	0.017
L-S	5 × 10 ¹⁹	-13	--	-11	68	12	0.679	0.012
L-T	0	-28	11		88	14		
T-L	0	-40	4		86	16		
T-S	0	-55	7		83	12		

^aWith respect to the base metal where L is the rolling as well as the welding direction.

Table 4. Effect of irradiation on the initiation toughness and tearing modulus of three-wire stainless steel cladding

Specimen	Test temperature (°C)	Modified J (ref. 12)		Deformation J (ref. 11)	
		J _{Ic} (kJ/m ²)	Tearing modulus	J _{Ic} (kJ/m ²)	Tearing modulus
<u>Unirradiated specimens</u>					
A13G	-75	118	82	117	64
H2	-75	144	67	137	49
A15B	20	169	319	165	270
A13D	20	135	265	134	209
A10G	20	174	223	171	176
A10E	120	128	311	128	246
H5	120	118	289	119	229
H3	120	120	288	120	232
A13F ^a	120	159	449	159	359
H6	200	88	293	90	240
H4	200	111	285	111	231
A15D	288	78	316	77	267
A13C	288	68	192	66	170
H1	288	79	241	82	192
<u>Irradiated specimens</u>					
A15F	-75	78	50	78	40
A15G	-75	57	40	56	36
A13A	30	145	218	144	177
A15C	50	128	182	124	146
A10F	120	97	207	94	175
A15A	288	23	223	25	191

^aThis specimen was not side-grooved while all other specimens in table were side-grooved 20%. This specimen was not included in the figures of J_{Ic} or tearing modulus vs test temperature.

LIST OF FIGURES

Fig. 1. Location of the Charpy specimens in the single-wire stainless steel cladding, nominally called type 308 and 309.

Fig. 2. Microstructure of three-wire stainless steel cladding weld overlay is typical of good quality commercial reactor pressure vessel cladding with delta-ferrite in austenitic matrix. Ferrite number ranges from about 7.5 to 10 in the three-layer cladding of this study.

Fig. 3. Effect of irradiation on the Charpy impact energy of type 308 stainless steel cladding.

Fig. 4. Effect of irradiation on the Charpy impact energy of high- and low-energy populations of the specimens of nominal type 309 cladding.

Fig. 5. Effect of specimen orientation on unirradiated tensile properties of three-wire stainless steel cladding. (a) Yield strength vs temperature. (b) Ultimate strength vs temperature. (c) Total elongation vs temperature.

Fig. 6. Unirradiated three-wire stainless steel cladding shows Charpy impact transition behavior. (a) CVN energy vs temperature, L-S orientation. (b) Effect of specimen orientation on CVN energy curves.

Fig. 7. Fracture surfaces of unirradiated three-wire stainless steel cladding CVN specimens tested at Charpy upper- and lower-shelf temperatures.

Fig. 8. Scanning electron microscopic examination demonstrates that fracture of stainless steel cladding is matrix controlled at the upper shelf and ferrite controlled at lower temperatures.

Fig. 9. Effect of neutron irradiation at 288°C on the yield strength of three-wire stainless steel cladding (yield strength vs test temperature).

Fig. 10. Effect of irradiation on the ultimate strength and elongation of three-wire stainless steel cladding. (a) Ultimate strength vs temperature. (b) Total elongation vs temperature.

Fig. 11. Effect of irradiation on the Charpy impact toughness of three-wire stainless steel cladding. (a) Charpy transition temperature and upper-shelf energy show increasing degradation with increasing neutron fluence. (b) Increasing neutron fluence from 2 to 5×10^{19} neutrons/cm² (>1 MeV) resulted in further transition temperature shift.

Fig. 12. Effect of irradiation on the Charpy V-notch lateral expansion of three-wire stainless steel cladding.

Fig. 13. Effect of irradiation on J_{Ic} initiation fracture toughness (modified J-integral calculation).

Fig. 14. Effect of irradiation on tearing modulus (modified J-integral calculation).

Fig. 15. Effect of irradiation on the J-R (modified J-integral) curve for three-wire stainless steel cladding tested at 120°C.

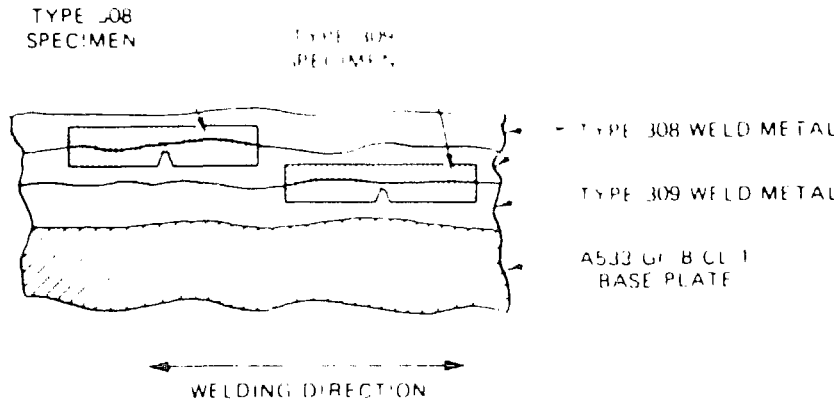


Fig. 1. Location of the Charpy specimens in the single-wire stainless steel cladding, nominally called type 308 and 309.

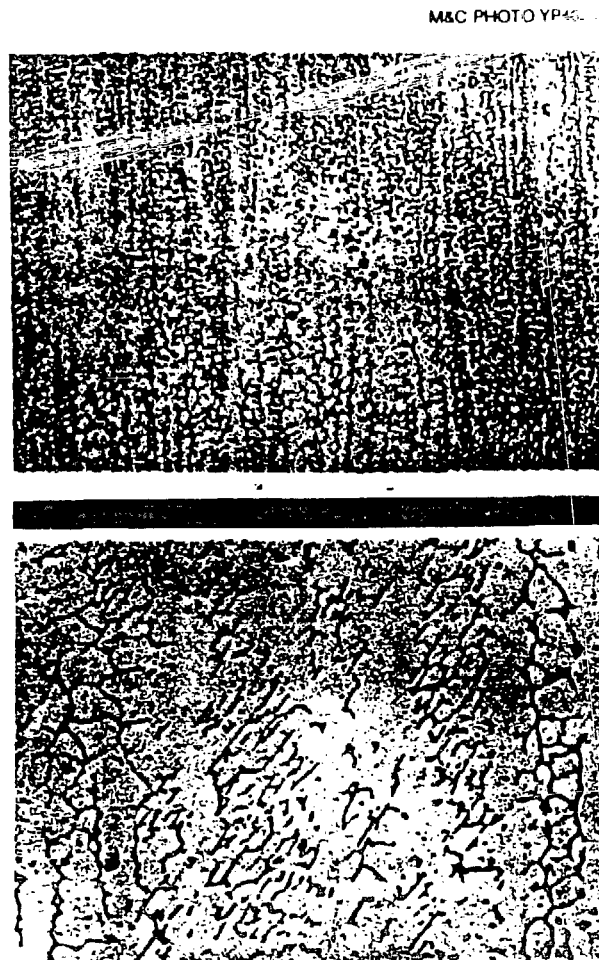


Fig. 2. Microstructure of three-wire stainless steel cladding weld overlay is typical of good quality commercial reactor pressure vessel cladding with delta-ferrite in austenitic matrix. Ferrite number ranges from about 7.5 to 10 in the three-layer cladding of this study.

REPRODUCED FROM BEST
AVAILABLE COPY

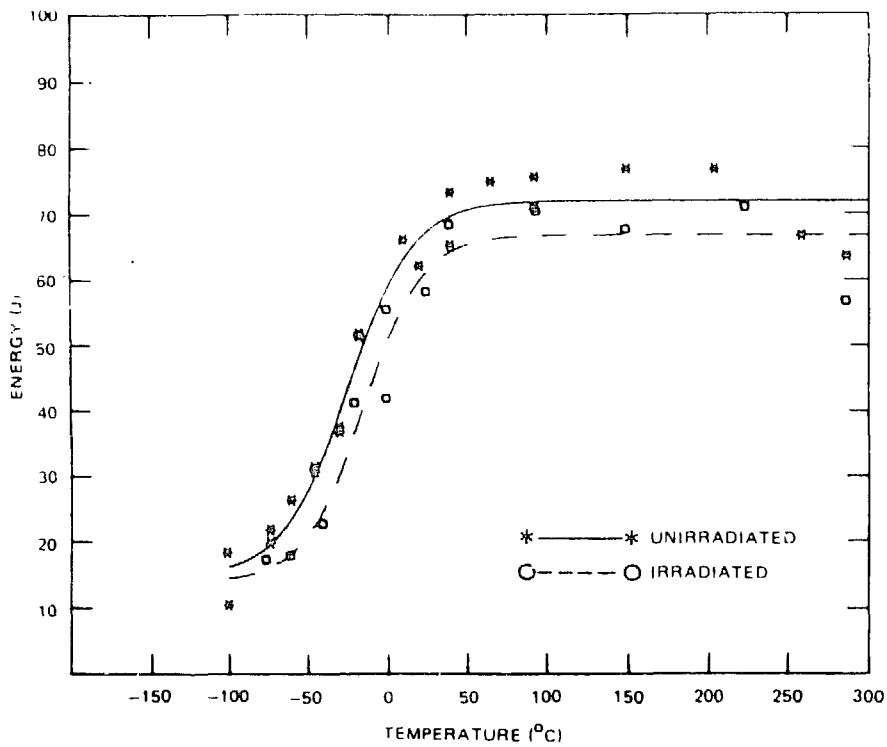


Fig. 3. Effect of irradiation on the Charpy impact energy of type 308 stainless steel cladding.

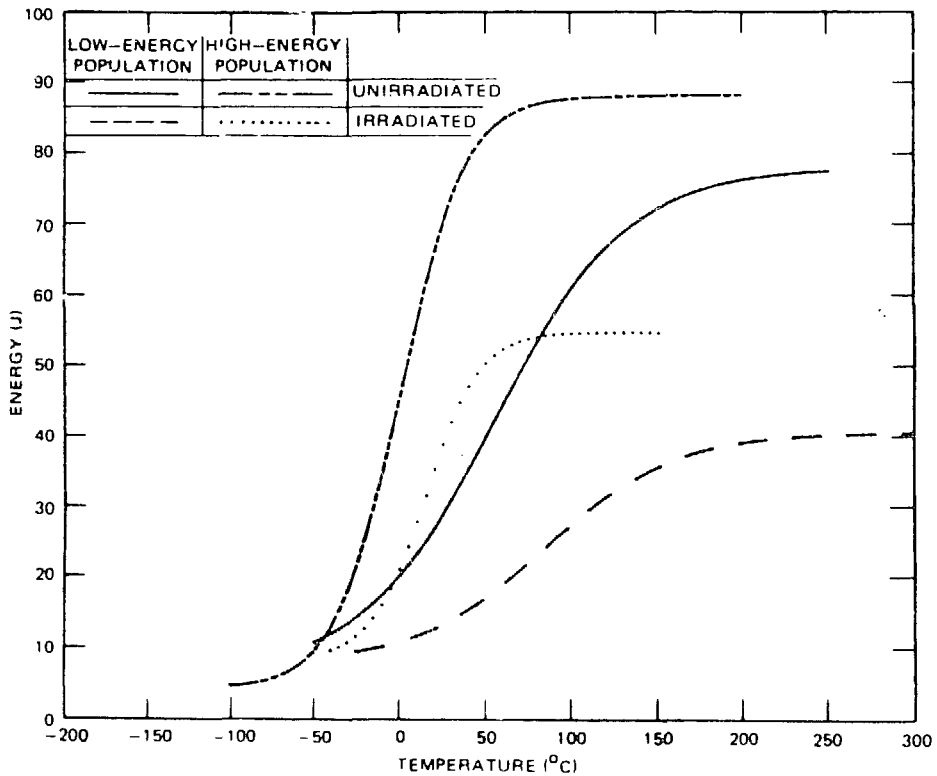


Fig. 4. Effect of irradiation on the Charpy impact energy of high- and low-energy populations of the specimens of nominal type 309 cladding.

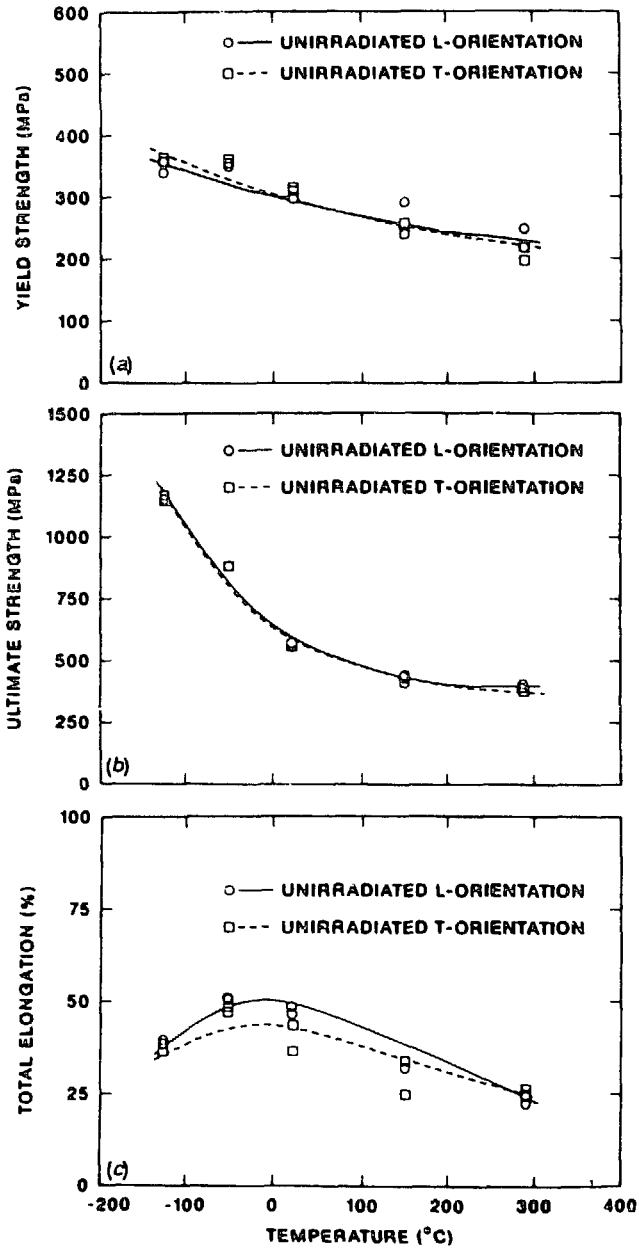


Fig. 5. Effect of specimen orientation on unirradiated tensile properties of three-wire stainless steel cladding. (a) Yield strength vs temperature. (b) Ultimate strength vs temperature. (c) Total elongation vs temperature.

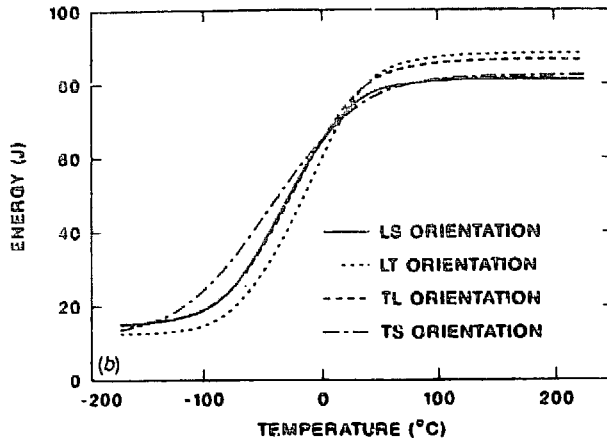
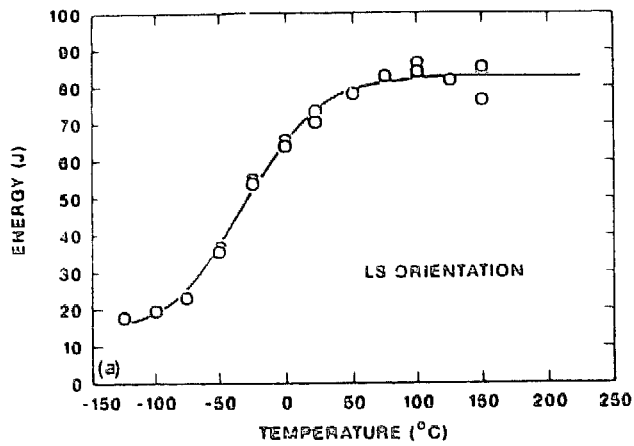


Fig. 6. Unirradiated three-wire stainless steel cladding shows Charpy impact transition behavior. (a) CVN energy vs temperature, L-S orientation. (b) Effect of specimen orientation on CVN energy curves.

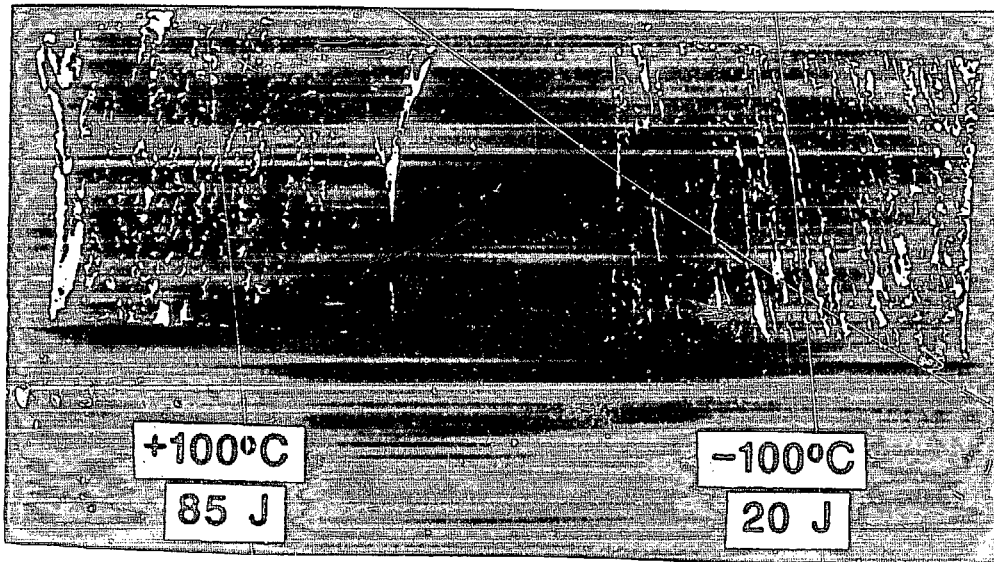


Fig. 7. Fracture surfaces of unirradiated three-wire stainless steel cladding CVN specimens tested at Charpy upper- and lower-shelf temperatures.

REPRODUCED FROM BEST
AVAILABLE COPY

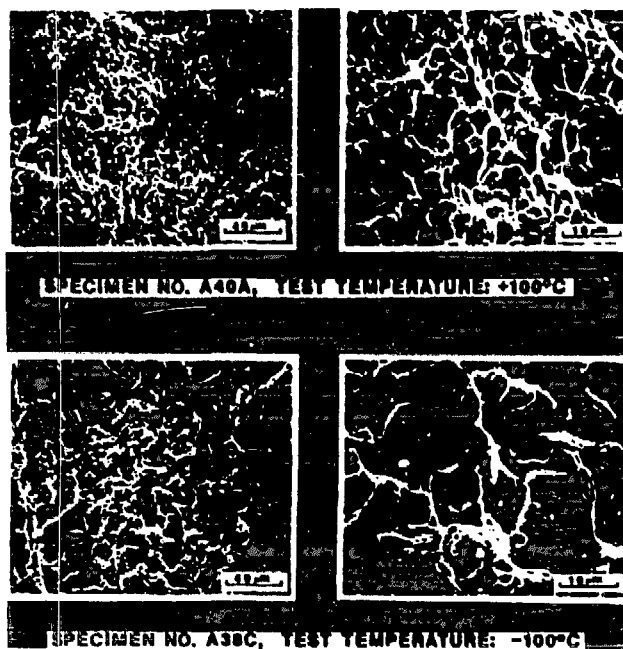


Fig. 8. Scanning electron microscopic examination demonstrates that fracture of stainless steel cladding is matrix controlled at the upper shelf and ferrite controlled at lower temperatures.

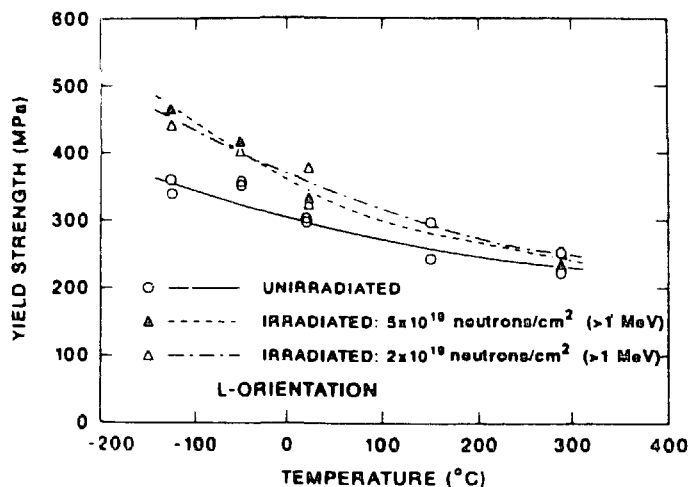


Fig. 9. Effect of neutron irradiation at 288°C on the yield strength of three-wire stainless steel cladding (yield strength vs test temperature).

REPRODUCED FROM BEST
AVAILABLE COPY

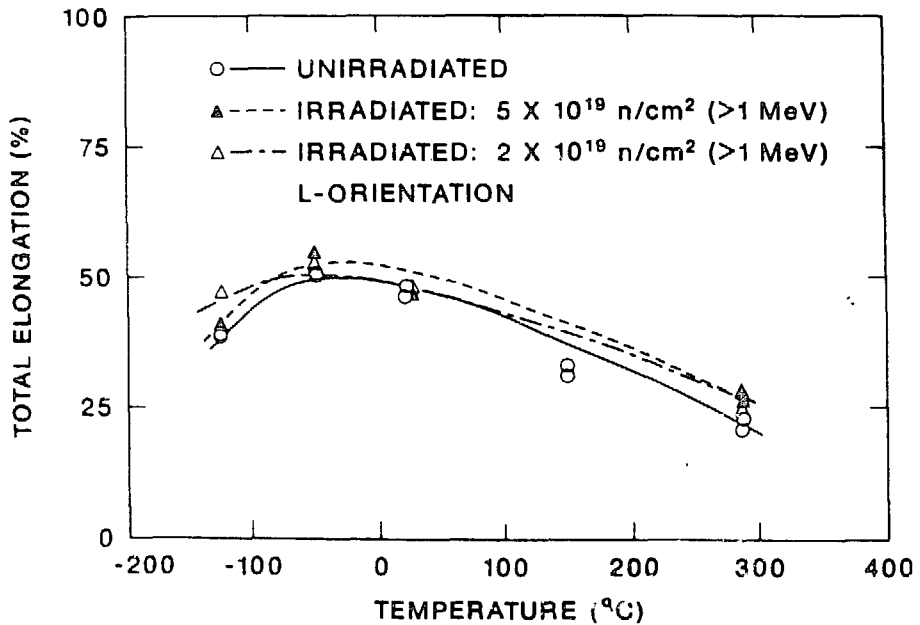
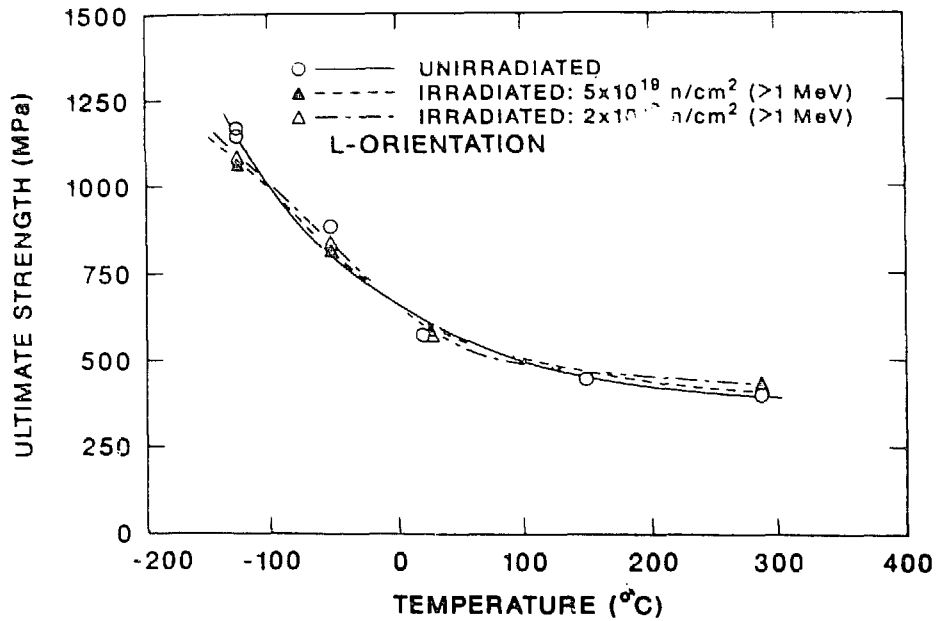


Fig. 10. Effect of irradiation on the ultimate strength and elongation of three-wire stainless steel cladding. (a) Ultimate strength vs temperature. (b) Total elongation vs temperature.

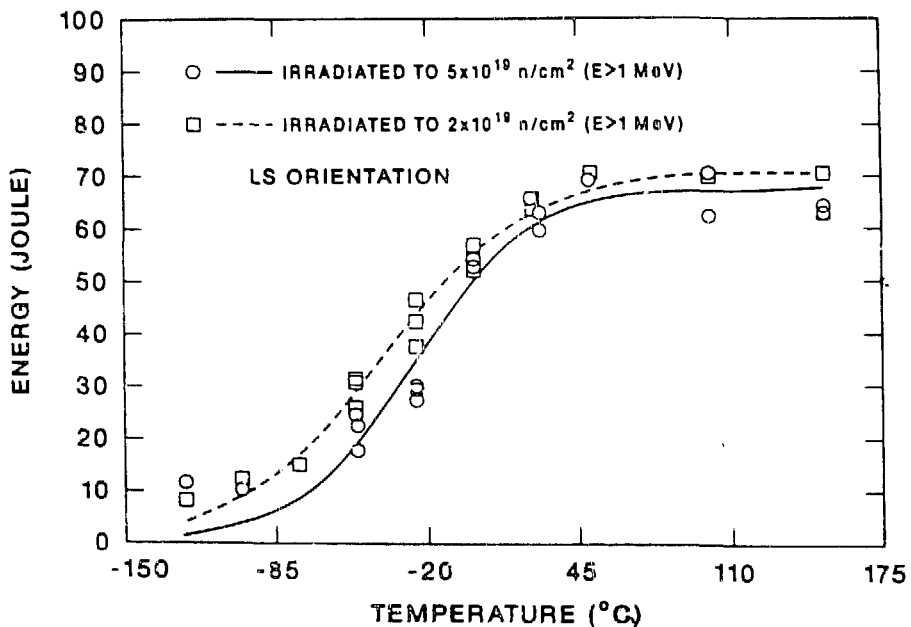
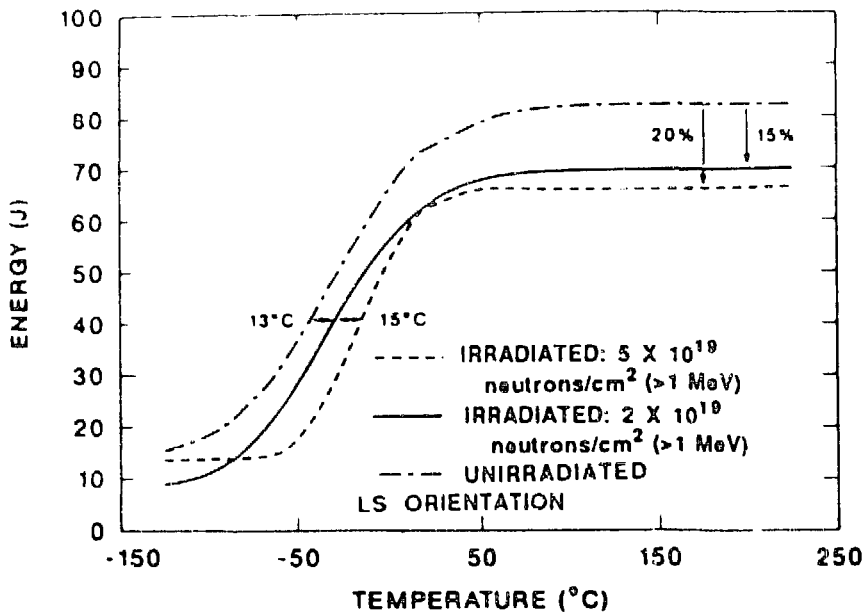


Fig. 11. Effect of irradiation on the Charpy impact toughness of three-wire stainless steel cladding. (a) Charpy transition temperature and upper-shelf energy show increasing degradation with increasing neutron fluence. (b) Increasing neutron fluence from 2 to 5 x 10¹⁹ neutrons/cm² (>1 MeV) resulted in further transition temperature shift.

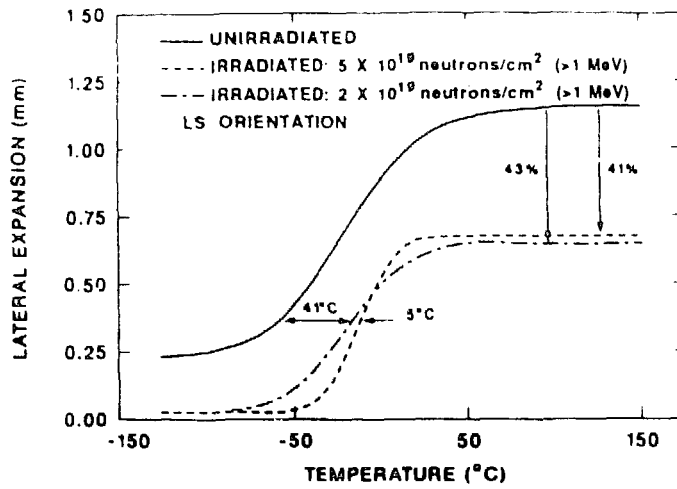


Fig. 12. Effect of irradiation on the Charpy V-notch lateral expansion of three-wire stainless steel cladding.

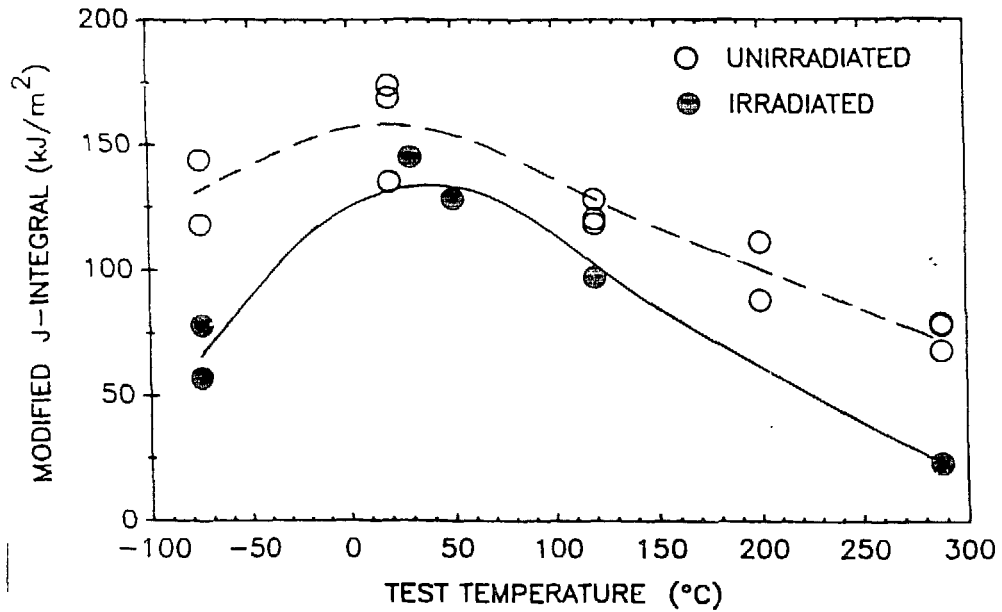


Fig. 13. Effect of irradiation on J_{Ic} initiation fracture toughness (modified J-integral calculation).

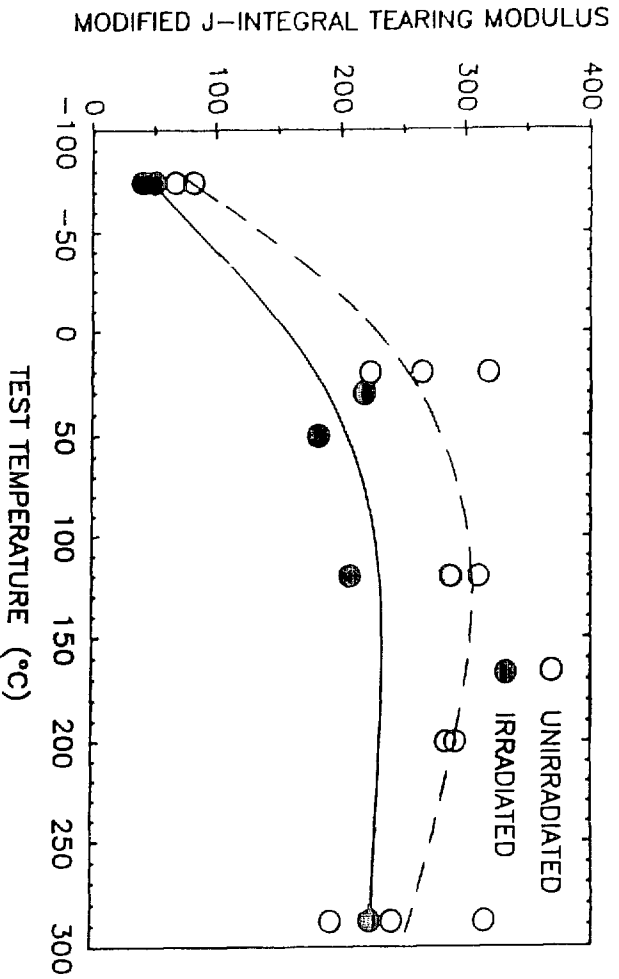


Fig. 14. Effect of irradiation on tearing modulus (modified J-Integral calculation).

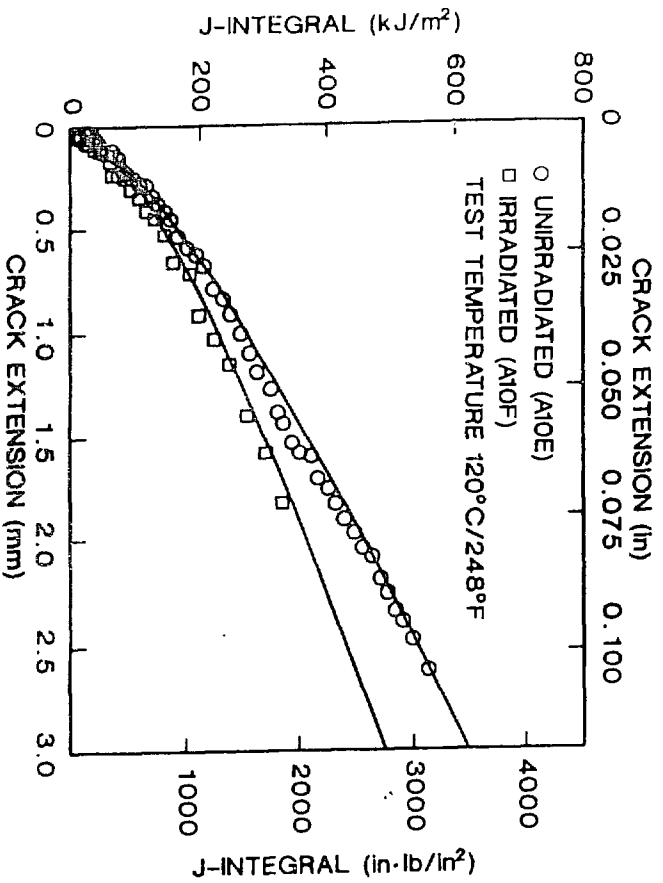


Fig. 15. Effect of irradiation on the J-R (modified J-Integral) curve for three-wire stainless steel cladding tested at 120°C.